Sensors and Actuators B 241 (2017) 466–472

Contents lists available at ScienceDirect

Sensors and Actuators B: Chemical

journal homepage: www.elsevier.com/locate/snb

Electroactive biofilms as sensor for volatile fatty acids: Cross sensitivity, response dynamics, latency and stability

Jörg Kretzschmar[a], Christin Koch[b], Jan Liebetrau[a], Michael Mertig[c,d], Falk Harnisch[b,*]

[a] DBFZ Deutsches Biomasseforschungszentrum gemeinnützige GmbH, Biochemical Conversion Department, Torgauer Straße 116, 04347 Leipzig, Germany
[b] Helmholtz-Centre for Environmental Research GmbH—UFZ, Department of Environmental Microbiology, Permoserstraße 15, 04318 Leipzig, Germany
[c] Technische Universität Dresden, Physical Chemistry, Measurement and Sensor Technology, 01062 Dresden, Germany
[d] Kurt-Schwabe-Institut für Mess- und Sensortechnik e.V. Meinsberg, Kurt-Schwabe-Str. 4, 04736 Waldheim, Germany

ARTICLE INFO

Article history:
Received 5 September 2016
Received in revised form 15 October 2016
Accepted 20 October 2016
Available online 21 October 2016

Keywords:
Microbial electrochemical technology
Bioelectrochemical systems
Biosensor
Geobacter

ABSTRACT

Microbial electrochemical sensors are an evolving technology platform based on electroactive microorganisms. Sensors based on anodic biofilms that oxidize organic substrates like acetate as living recognition element are promising for online monitoring of anaerobic digestion (AD), wastewater treatment as well as other processes. Essential for future engineering of microbial electrochemical sensors is the detailed characterization of its cross sensitivity as well as response behavior and latency. These parameters were examined on the example of a microbial electrochemical acetate sensor build in a 100 mL continuously stirred tank reactor. Furthermore, the ability of the sensor to recover after different periods (5–10 days) of shut down (i.e. open cell potential (OCP)) was studied. The sensor showed cross sensitivity towards propionate and butyrate that can be described as a baseline sum signal (0.040 ± 0.008 mA cm^{-2}) irrespective of the applied concentration. The sensor also revealed biphasic response behavior towards dynamic changes in acetate concentration shown to be strongly dependent on prior exposure to low acetate concentrations. This behavior is discussed by means of the metabolic state of the microbial cells forming the recognition element. Furthermore, the sensor revealed full recovery of activity after three consecutive OCP periods showing that sensor shutdown is not a limiting factor. The dynamic response behavior and the cross sensitivity of the sensor are discussed as challenges for engineering of future applications.

1. Introduction

Microbial electrochemical technologies (MET) are a promising technology platform of increasing interest. Primary MET are based on the ability of electroactive microorganisms to use electrodes as electron acceptors or donors [1,2]. This interaction can either be based on direct [3–6] or mediated [4,7] extracellular electron transfer. The microbial fuel cell (MFC), an electric power producing device, is the archetype of MET. In a MFC an anodic biofilm composed of electroactive microorganisms oxidizes organic compounds of, e.g. wastewater, to CO_2 and protons while transferring electrons to the electrode. Other applications comprise microbial electrochemical sensors. In microbial electrochemical sensors the permanent connection of the microbial metabolism and the electrode is used for generating an analytical signal, e.g. using the electric current as measure of cellular respiration, and hence, as measure of concentration of the microbial substrate. Most promising are sensors for the detection of volatile fatty acids (VFA) in biotechnological processes like wastewater treatment or anaerobic digestion (AD) for biogas production [8–13]. As there are no cost efficient sensors for monitoring VFA in AD plants available, this study focuses on the latter. During AD macromolecules are broken down to methane by four microbiological steps, namely hydrolysis, acidogenesis, acetogenesis and methanogenesis [14]. Acetogenic bacteria that perform acetogenesis live in a strong syntrophic relationship with the methanogenic archaea, as they consume the H_2 produced by the acetogens whereby acetate production is made energetically feasible [15,16]. Process imbalances leading to the inhibition of methanogenesis result in an accumulation of VFA, most important acetate that in turn inhibits the involved microorganisms and can hence cause process breakdown [17–20]. Running anaerobic digestion at high or varying loading rates, e.g., for flexible biogas production as a tool of power grid management [21–23], requires monitoring VFA concentrations to avoid the risk of process acidification and breakdown. Here we will demonstrate that the required highly time resolved VFA measurement can be accom-

* Corresponding author.
E-mail address: falk.harnisch@ufz.de (F. Harnisch).

http://dx.doi.org/10.1016/j.snb.2016.10.097

plished by a microbial electrochemical sensor. The sensor is based on a naturally grown anodic *Geobacter* sp. dominated biofilm as recognition element, i.e. receptor that has been demonstrated to deliver an amperometric biosensor signal (oxidation current correlating to the concentration of acetate [13]).

Transferring such a technology concept from the laboratory scale to real application is challenging. One key challenge is related to different and especially changing environmental conditions affecting the involved electroactive microorganisms [24–28]. It was shown that changing salinity, pH, temperature as well as substrate concentrations influences the activity and stability of electroactive biofilms [29–33]. Fluctuations in the environmental conditions, however, contradict with the strong need for specificity, reproducibility and stability of the sensor. Thus, a stable or at least predictable performance while facing changing environmental conditions is a basic prerequisite.

For a better understanding of the response behavior of the sensor in the light of its proposed application for AD-monitoring, this work describes the following exemplary key challenges. When moving from an acetate based laboratory setup to a real application it is of particular interest to examine: I) the cross sensitivity towards different VFA, II) the response dynamics and latency (*i.e.*the delay in time of the measured sensor signal compared to a signal that occurs without any lag of time) caused by different acetate provision rates and incubation times at low acetate concentration, and III) the stability of the biofilm when shutting down the sensor, i.e. incubation of the electroactive biofilms at open cell potential (OCP), and its effect on sensor functionality.

2. Material and methods

All chemicals were of analytical or biochemical grade and purchased from Carl Roth GmbH (Germany) and ChemSolute (Th. Geyer GmbH & Co. KG, Germany). If not stated otherwise, all potentials provided in this article refer to the Ag/AgCl reference electrode (sat. KCl, 0.197 V vs. standard hydrogen electrode (SHE)).

2.1. General experimental setup and operation

All working and counter electrodes, with a geometric surface area of 3.34 cm^2 and 4.12 cm^2, respectively, were made from carbon rods with a diameter of 0.5 cm (CP-Handels-GmbH, Germany).

Each experiment was conducted in a flow cell setup consisting of a 100 mL continuously stirred tank reactor (CSTR) type vessel (n = 3) possessing three ports for electrodes (working, counter and reference electrode) as well as inlet and outlet for substrate feeding and removal, respectively [13]. The growth medium was based on 50 mM phosphate buffer supplemented with trace elements and vitamins as described elsewhere [34,35]. It differed in concentration and type of the analyte that also represents the sole carbon source (see specific descriptions of the single experiments below). The medium was provided with a peristaltic pump (TU 200, Medorex e.K., Germany) and air-tight Tygon tubes (E 3603, Saint – Gobain Performance Plastics, France) at different flow rates.

All experiments were conducted at 38 °C (Incubator Hood TH 15, Edmund Bühler GmbH, Germany) at constant stirrer speed of 250 rpm using a magnetic stirrer. The headspace of the 5 L storage tank was continuously flushed with nitrogen. For the experiments described below secondary, electroactive anodic biofilms [36] were grown in batch mode according to [35] using acetate as sole substrate. Once the first batch of substrate was depleted the experimental setup was switched to continuous flow mode [13]. Only for the examination of the biofilms cross sensitivity towards different VFA, an equimolar mixture of butyrate, propionate and acetate was used for the biofilm formation (see Section "VFA cross sensitivity and structure of the microbial community"). The term "secondary biofilms" implies the use of established primary biofilms from wastewater as inoculum for the biofilm formation and represents an established enrichment method for electroactive microorganisms [36].

Electrochemical measurements were always performed with a multipotentiostat (PARSTAT MC, AMETEK Inc., USA) using the following electrochemical techniques: chronoamperometry (CA) at 0.2 V and cyclic voltammetry (CV) with a scan rate of 1 mV s^{-1} and vertex potentials at 0.3 V and −0.5 V. In case of CV measurements, three cycles were performed with only the last cycle being used for data analysis. The use of CV measurements allows a detailed monitoring of the dynamic current response of the biofilms at different potential whereas CA measurement provides the current density at a fixed potential, i.e. electrochemical driving force.

2.2. VFA cross sensitivity and structure of the microbial community

For this set of experiments, the formation of the secondary electroactive anodic biofilms was conducted with a 5 mmol L^{-1} equimolar mixture of acetate, propionate and butyrate. To subsequently examine the cross sensitivity of the biofilms, acetate, propionate and butyrate were applied as single analyte as well as in equimolar mixture. Altogether, four different concentration steps (0.5, 1, 2 and 4 mmol L^{-1}) were each applied for ~25 h at a constant flow rate of 1 mL min^{-1} (hydraulic retention time: 100 min). CA measurements were performed for 23 h followed by CV. Biofilm samples were taken at the end of the experiments with a spatula and stored at −18 °C until microbial community analysis (T-RFLP and sequencing, see Section "Microbial community analysis") was performed.

2.3. Analysis of response behavior and latency

For this set of experiments, the biofilms were grown with 10 mmol L^{-1} acetate as sole substrate. To characterize the response behavior of the biofilms, two experimental settings were investigated: I) response to different acetate concentrations (2 and 3 mmol L^{-1}) pumped with varying flow rates and II) response to a stable final acetate concentration (4 mmol L^{-1}) pumped with a stable flow rate but varying initial incubation times at defined lower acetate concentrations (1 and 2 mmol L^{-1}).

For the first setting, 2 and 3 mmol L^{-1} acetate was added to the experimental setup with different flow rates (1, 2, 3, 4, or 5 mL min^{-1}) each. At the start of the experiment the growth medium in the experimental setup contained no acetate. The biofilms were always provided with 5 L of growth medium per experimental run. The flow rate in combination with the 5 L volume storage tank defined different experiment durations ranging from 5.5 h for 5 mL min^{-1} to 27.7 h for 1 mL min^{-1}. The biofilm response was measured with CA at 0.2 V.

For the second experimental setting, the flow rate remained stable at 3 mL min^{-1} and the sensor was set to a low initial acetate concentration (1 and 2 mmol L^{-1}) for two defined periods (3 and 24 h). The final acetate concentration was raised to 4 mmol L^{-1} acetate to keep the concentration difference stable compared to the fist experimental setup. For data acquisition, CA measurement at 0.2 V was performed. To detect any deviation from an ideal and latency free response of the biofilms, the current density (sensor signal) measured in the experiments was compared to the calculated acetate concentration for an ideal CSTR [13]. Furthermore, the t_{95} for the experimental setup, i.e. the time needed to reach 95 % of the maximum current density, and the sensor latency was determined (see Section "Data and statistical analysis").

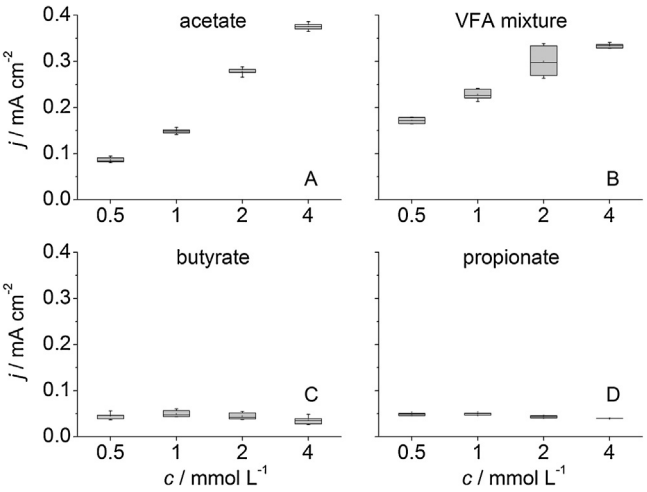

Fig. 1. Cross sensitivity of electroactive biofilms. The graphs show the biofilm response on changing VFA concentrations. The data was summarized from CA and CV measurements. The grey boxes correspond to the middle 50% of the data, whiskers (error bars) indicate minimum and maximum, n = 3.

2.4. Stability of electroactive biofilms towards OCP periods

The ability of electroactive biofilms to recover to full activity after a defined period at OCP, i.e. absence of electron acceptor, was tested by switching the experimental setup with established secondary biofilms grown on 1 mmol L^{-1} acetate from 0.2 V to OCP for 10 days. Thereafter, the CA measurement was restarted with fresh medium at the same acetate concentration level as before until stable current production occurred for at least 1000 min. This procedure was repeated for another 5 and 6 days OCP after 22–33 h of constant operation. For data analysis, only the last 1000 min of stable CA measurement were used.

2.5. Data and statistical analysis

All measurements in this study were performed as independent triplicates.

The current density data from the VFA cross sensitivity experiment were evaluated graphically in a quartile based box plot (Fig. 1). Therefore, the average current density of stable CA measurement (last 600 min or 200 data points, respectively, for every applied analyte concentration) was combined in one data set with the current density measured with CV at 0.2 V (average of forward and backward scan), see also [13].

To detect any deviation from an ideal and latency free response of the biofilms, the current density measured in the response behavior experiments were compared to the calculated acetate concentration according to Eq. (1), describing the experimental setup as continuously stirred tank reactor (CSTR) as already validated in [13].

$$C = C_0 * (1 - e^{\frac{-t}{t_g}}) \quad (1)$$

With C: concentration at time t, C_0: final concentration, t_g: mean hydraulic retention time of the flow cell (100 min). The t_{95} calculated for the sensor setup differs from the common calculation of this parameter that describes the time a sensor needs to reach 95% of the maximum signal if exposed to constant analyte concentration. Here we refer to a flow cell setup with a dynamic analyte concentration. Hence, the value gained is not the t_{95} by strict definition. However, we suppose it is still providing valuable information and does rather overestimate the value. It is determined from the point where the final acetate concentration (4 mmol L^{-1}) was initially applied to the flow cells and not from the time where the bulk acetate concentration in the flow cells reached 4 mmol L^{-1}.

The latency of the sensor represents the delay in time of the real sensor signal (caused by the change of experimental parameters) compared to a signal that represents a response to a change of analyte concentration occurring without any lag of time. The latency was calculated as time difference between the time to reach 95% of the maximum current density measured in the flow cell setup (t_{95real}) and the calculated value (t_{95calc}) using the ideal CSTR model, i.e. a latency free signal.

To compare more than two current density data sets at once (200 data points per data set), Kruskal Wallis test with post hoc Dunn-Bonferroni test was performed (SPSS Statistics 20 software, IBM). The tests were chosen because Kolmogorov Smirnov test rejected normal data distribution. Pairwise comparison of data sets was conducted with the Mann Whitney test (Origin 9.1 software, Origin Lab). The α-level was set to 0.05 in all cases.

2.6. Microbial community analysis

Microbial community analysis was performed on DNA level to determine changes of the anodic biofilm community due to changes in the analyte (VFA cross sensitivity experiments). Biofilm samples were taken at the end of the experiments with a spatula and stored at −18 °C. DNA extraction was performed with the NucleoSpin Soil® kit (Macherey-Nagel) following the manufacturer's instruction. Terminal restriction fragment length polymorphism (T-RFLP) analysis, cloning and sequencing were based on partial amplification of the 16S rRNA gene according to standard procedures as described elsewhere [37]. PCR was performed with the Fluorescein amidite (FAM)-labeled primer set UniBac27f and Univ1492r, and restriction digestion using *Rsa*I and *Hae*III.

3. Results and discussion

3.1. VFA cross sensitivity and structure of the microbial community

The secondary biofilms for this experiment were grown with a 5 mmol L^{-1} equimolar mixture of acetate, butyrate and propionate in batch mode for 3 days followed by additional 17 days in flow mode. At day 13 the biofilms produced a steady state current density of 0.569 ± 0.013 mA cm^{-2}. This is in line with former measurements as well as literature data for anode biofilms with acetate as sole substrate [38,30,13].

The specificity of a sensor is defined as its cross sensitivity towards interfering components under operating conditions. The term interfering components relates to components that can either reduce the sensor signal because of, e.g. toxic properties, or increase the sensor signal, e.g., as they represent an alternative substrate for the electroactive bacteria. During AD different VFAs can be present, and hence, can interfere with the electroactive biofilm, and in turn, affect the sensor signal. Fig. 1 shows the biofilm current density, serving as sensor signal, derived from CA and CV measurements for acetate, propionate, butyrate and equimolar mixtures thereof. In a concentration range from 1 to 4 mmol L^{-1}, the current density shows a proportional dependency to the applied acetate concentration (Fig. 1A). The concentration range was chosen as the sensor setup features a measurement range from 0.5 to 5 mmol L^{-1} acetate (Kretzschmar et al. [13]). For propionate and butyrate, the current density in Fig. 1 are significantly lower for all applied concentration steps and seem to reveal a baseline signal in the range of 0.038–0.054 mA cm^{-2} irrespective of the applied concentration. A reference measurement without any analyte, hence C-source, lead to an average signal of 0.024 ± 0.006 mA cm^{-2} over

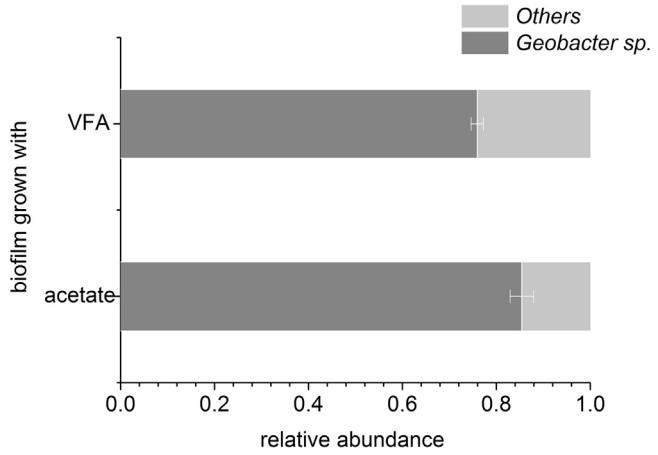

Fig. 2. Microbial community analysis of biofilms grown with different VFAs based on T-RFLP analysis. *Geobacter* sp. dominates the electroactive biofilm communities grown on acetate as sole carbon source or a VFA mixture consisting of acetate, propionate and butyrate. Error bars indicate standard deviation, n = 3.

a period of 600 min, revealing clearly that butyrate and propionate cause a metabolic reaction within the biofilms. An average baseline signal for propionate and butyrate can be calculated as 0.040 ± 0.008 mA cm^{-2} for all applied concentration steps. The current density achieved when applying an equimolar mixture of all VFAs is shown in Fig. 1B. The obtained value for the VFA mixture, e.g. 0.269 ± 0.015 mA cm^{-2} at 2 mmol L^{-1}, is almost identical to the current density obtained, when summing up the current densities of the individual experiments, e.g. at 2 mmol L^{-1} from Fig. 1A, C and D yields 0.271 ± 0.011 mA cm^{-2}. Therefore, the biofilm sensor is shown to yield a sum signal consisting of individual signals from each analyte. The baseline signal for butyrate and propionate reveals that the sensor cannot be used for detecting both VFAs quantitatively in the applied concentration range. Nevertheless, statistical analysis revealed significant differences between 0.5 and 2 mmol L^{-1} butyrate (Kruskal Wallis test) as well as between butyrate and propionate each for the same applied concentration (pairwise comparison, Mann Whitney test). This implies that the sensor can be used to detect butyrate or propionate each as sole analyte which, thus, improves its practical relevance. In a previous study the measurement resolution for the applied sensor setup was determined between 0.25 and 1 mmol L^{-1} acetate, depending on the applied acetate concentration [13]. Hence, the differences in measurement resolution of the current density for acetate (see also Fig. 1A) are higher than the differences in current density obtained for butyrate and propionate obtained across the whole applied concentration range (Fig. 1C and D). This means, the sum signal for all three analytes is within the described measurement resolution (Fig. 1B), irrespective of the statistical differences of the partial signals. However, the previously described measurement range from 0.5 to 5 mmol L^{-1} acetate [13] is reduced for the equimolar mix of analytes (Fig. 1B), as signal saturation occurs already at concentrations higher than 2 mmol L^{-1} VFA mixture.

To evaluate if the different VFAs have an influence on the community structure of the electroactive biofilms, T-RFLP analysis and sequencing were carried out. Fig. 2 shows the dominance of *Geobacter* sp. in the anodic biofilms grown at 0.2 V in accordance with previous experiments [39,40,37]. Based on BLAST comparison, this strain is most closely related to *Geobacter anodireducens* strain SD-1 (CP014963.1, 99% identity, 100% query coverage). All T-RFs with different affiliation were summed up and denominated as "Others". The dominance (75–88 %) of *Geobacter* sp. in the anodic biofilms is independent of the applied VFAs, as slight abundance differences are in the range of methodical variation.

3.2. Response behavior of electroactive biofilms

The latency of a biosensor is one of its key characteristics. In a previous work we demonstrated the latency free response of the experimental setup for a concentration step from 0 to 0.5 mmol L^{-1} acetate and a flow rate of 1 mL min^{-1} [13]. This concentration step is too low for the designated practical application, so the latency of acetate grown biofilms was systematically studied up to a total range of 3 mmol L^{-1} acetate. The secondary biofilms for this experiment were grown with 10 mmol L^{-1} acetate in batch mode for 6 days followed by additional 16 days in flow mode. Fig. 3 shows the response on acetate concentration steps from 0 to 2 and 0 to 3 mmol L^{-1} acetate with flow rates varying from 1 to 5 mL min^{-1}. In all cases, the trend of the current density responses of the biofilms deviated from the expected single-phase saturation behavior, previously reported [13]. While for a flow rate of 1 mL min^{-1}, only small changes from the single phase saturation behavior occurs, higher flow rates (2–5 mL min^{-1}) lead to a biphasic trend in current density. For all conditions, a second activity phase starts after ~100 min. Most important, this occurs irrespective of the applied flow rate indicating that the bulk acetate concentration is not deterministic for the biphasic response. Increasing the flow rates intensifies the biphasic response whereas slower flow rates (1–2 mL min^{-1}) cause smaller deviations from a single phase saturation behavior. For better visualization, the time point of acetate saturation in the experimental setup (calculated according to an ideal CSTR) is marked with vertical, dotted lines in Fig. 3 for every applied flow rate. If the bulk acetate concentration would be responsible for the biphasic behavior, the phase shift would occur at different points in time. Hence, it would be individual for each flow rate and not occur at the same point in time.

The origin of the biphasic response behavior does not rely on the bulk acetate concentration, so further parameters were investigated. The duration of the incubation at low acetate concentrations (1 mmol L^{-1} or 2 mmol L^{-1}) was varied (3 h, 24 h) before increasing acetate to a concentration of 4 mmol L^{-1}. Fig. 4A shows the concentration step from 1 to 4 mmol L^{-1} acetate. Irrespective of the incubation time, both signals reach saturation slower than calculated for an ideal CSTR (red dotted line in Fig. 4). For the smaller concentration step from 2 to 4 mmol L^{-1} acetate (Fig. 4B), the deviation from the ideal CSTR behavior is different. The short period at 2 mmol L^{-1} acetate caused an even faster response to the concentration step to 4 mmol L^{-1} as the model predicts (black line in Fig. 4B). Obviously, the 24 h pre-treatment at 2 mmol L^{-1} acetate results in a slower saturation of the current density (blue line in Fig. 4B).

To quantify the deviation of the response behavior from the model, and therefore, to account for the effect of the incubation period with low acetate concentrations, the t_{95} (see Materials and methods Section) of the experimental setup was calculated for the concentration step from 1 to 4 mmol L^{-1} and 2 to 4 mmol L^{-1} acetate as well as for the model. Table 1 comprises the calculated t_{95} data. In every case, the t_{95real} values differ from the calculated values for ideal CSTR-conditions (t_{95calc}). Except for the short pretreatment period at 2 mmol L^{-1} acetate, every concentration step results in increased response latency between 73.2 ± 7.5 and 311.6 ± 10.2 min (2.3–4.5 fold increase of t_{95calc}). The biofilm response for the concentration step after preceding 3 h at 2 mmol L^{-1} acetate revealed a negative latency value of -27.08 ± 7.2 min (1.5 fold decrease of t_{95calc}).

The reasons for the observed biphasic response behavior and the related latency of the sensor remain unclear. From the authors' perspective, two hypotheses can be drawn.

First, the deviation can be caused by the metabolic state of the electroactive bacteria in the biofilm. Assuming that the enzymes needed for the oxidation of acetate are present at levels that are

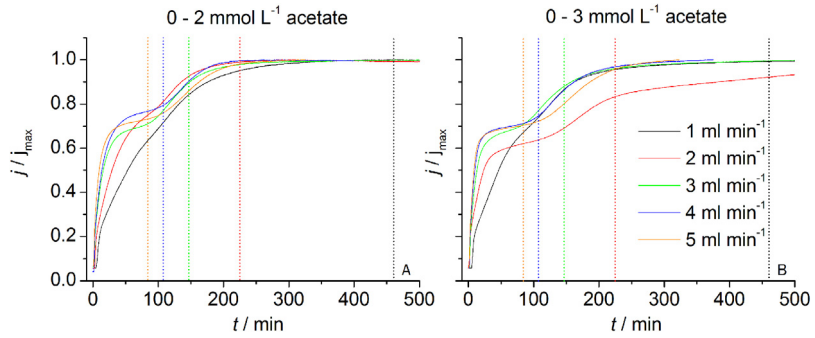

Fig. 3. Response behavior of electroactive biofilms. Current response (normalized to j_{max}) of electroactive biofilms on different acetate concentration steps applied with different flow rates. Vertical, dotted lines indicate calculated acetate saturation in the respective experimental flow cell setup. Acetate saturation was calculated according to an ideal CSTR, see also (Kretzschmar et al. [13]), n = 3.(For interpretation of the references to colour in this figure legend, the reader is referred to the web version of this article.)

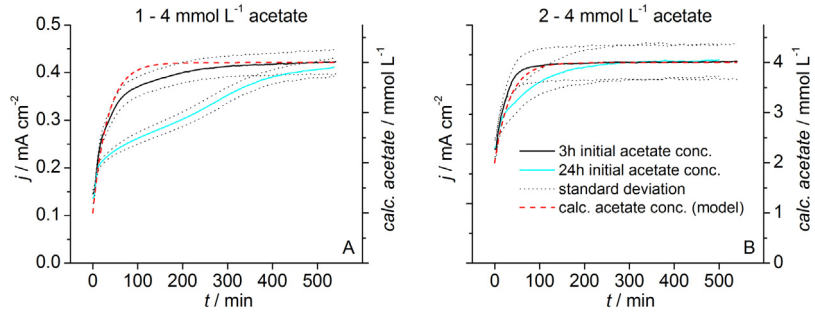

Fig. 4. Response behavior of electroactive biofilms as a function of two different incubation times and two different acetate concentration steps. The biofilm signals are influenced by the low acetate concentration during the incubation period: 3 h and 24 h at 1 mmol L^{-1} acetate (A) and 2 mmol L^{-1} acetate (B), respectively. The current density was compared to the expected current response based on the provided acetate concentration. The red dashed lines represent the calculated acetate concentration according to an ideal CSTR model, see also (Kretzschmar et al. [13]). Standard deviation of the current signal is represented by the black dotted lines, n = 3. (For interpretation of the references to colour in this figure legend, the reader is referred to the web version of this article.)

Table 1
Biofilm response behavior as a function of the incubation time at low acetate concentration prior the increase to 4 mmol L^{-1} acetate (flow rate: 3 mL min^{-1}). *t*: incubation time at low acetate concentration, j_{95}: 95 % of maximal current density, t_{95real}: time to reach 95 % of the maximal current density, t_{95calc}: calculated t_{95} for the ideal CSTR model, latency: difference of $t_{95real} - t_{95calc}$.

Parameter	1–4 mmol L^{-1} acetate		2–4 mmol L^{-1} acetate		Unit
t	3	24	3	24	h
j_{95}	0.403 ± 0.019	0.392 ± 0.015	0.419 ± 0.023	0.421 ± 0.022	mA cm^{-2}
t_{95real}	211.5 ± 10.2	401.9 ± 13.3	49.8 ± 7.2	150.0 ± 7.5	min
t_{95calc}	90.3	90.3	76.8	76.8	min
latency	121.3 ± 10.2	311.6 ± 10.2	−27.08 ± 7.2	73.2 ± 7.5	min

adjusted by the microbial cells, an increase of the acetate concentration would trigger their formation. However, if the acetate increase is faster than the microbial enzyme formation, latency in the biofilm response would occur as observed in Figs. 3 and 4. Obviously, the longer the biofilm is exposed to a certain concentration of acetate the better the metabolic state may be adjusted to it. The latter would also explain the fast response of the biofilms that remained only 3 h at a low acetate concentration (2 mmol L^{-1}), as the bacterial metabolism is still adapted to higher substrate concentration of, e.g. 4 mmol L^{-1}. It also accounts for the high observed t_{95} and high biofilm response latency for the acetate concentration step from 1 to 4 mmol L^{-1} or even no acetate (Fig. 3), as the bacterial metabolism has to adapt to a higher rate of substrate increase.

The second hypotheses is based on [41–43]. Yang et al. mention two reversible pathways of acetate oxidation in a *Geobacter soli* type that are detailed described in [41,42]. *Geobacter soli* may be a heterotypic synonym of *Geobacter anodireducens* that has been identified as the dominating phylotype in the biofilms described in this work as well as in other biofilm electrodes [44–46]. Aklujkar et al. [42] assume that the occurrence of two pathways for acetate activation with coenzyme A may indicate inefficient acetate utilization at low acetate concentrations. This hypothesis could also explain the biphasic behavior observed in our experiments.

3.3. Stability of electroactive biofilms towards different OCP periods

The recovery of electroactive anodic biofilms after phases of inactivity was tested by switching the anodic potential from 0.2 V to OCP for several days. For biosensor applications, this procedure is comparable to technical failures or maintenance procedures. The secondary biofilms used for this experiment were grown on acetate as sole substrate. Altogether, three consecutive OCP periods with duration of 10, 6 and 5 days were conducted. The biofilms could always recover full and stable activity with current densities from 0.233 to 0.243 mA cm^{-2} using 1 mmol L^{-1} acetate. The data possessed significant differences for two of three groups (Kruskal Wallis test, each group containing 200 data points) but were always within the measurement resolution of the experimental setup of 0.25–1 mmol L^{-1} acetate [13]. These results show that *Geobacter*

anodireducens dominated biofilms can withstand periods of up to 10 consecutive days and 21 days in sum at OCP, i.e. without electroactive metabolic activity. The biofilms metabolic capability was not affected by this procedure. The observed recovery of the biofilms is a good basis for technical applications where technical failures can occur.

4. Conclusion

In this study a microbial electrochemical acetate sensor was characterized with regards to its cross sensitivity and related effects on the microbial community of the recognition element (electroactive biofilm), its response behavior on dynamic analyte supply as well as its latency and functional stability.

When providing acetate, butyrate and propionate in equimolar mixture, the sensor generated a sum signal that was dominated by acetate whereas butyrate and propionate contributed as additive baseline signals irrespective of the applied concentration. Applying the VFA mixture also resulted in a reduction of the upper measurement range limit from 5 mmol L^{-1} for acetate [13] to 2 mmol L^{-1} for the VFA mixture. Hence, the sensor can be considered more appropriate as a VFA sensor with acetate as the main analyte. If solutions with only one specific VFA are of analytical interest, the sensor may also be able to detect propionate or butyrate alone. Although butyrate and propionate caused changes in the sensor signal compared to experiments with acetate as sole analyte, the composition of microbial community of the recognition element was not affected and remained stable. However, for longer time periods there might be metabolic as well as community shifts with both aspects needing further investigation.

The sensor response to dynamic acetate supply revealed a dependency from: 1) the incubation time at low acetate concentration prior to a concentration step, and 2) the extend of the following concentration step. A long incubation time (e.g. 24 h) at low concentrations (0–2 mmol L^{-1} acetate) resulted in a reproducible biphasic response behavior that can be minimized or avoided by reducing the incubation time at low concentrations. Consequently, the latency of the sensor is increased or reduced depending on the initial incubation time at low acetate concentrations. Concerning an initial acetate concentration of 1 mmol L^{-1} for 24 h followed by a concentration increase to 4 mmol L^{-1}, the sensor latency increased to 311.6 ± 10.2 min. However, an initial acetate concentration of 2 mmol L^{-1} for 3 h followed by a concentration increase to 4 mmol L^{-1} reduces the sensor latency to -27.08 ± 7.2 min. The reason for the biphasic behavior, and therefore, observed latency remains unclear but it is conceivable that the metabolic state of the electroactive microorganisms is responsible, either by adjusting the level of the required enzymes or by the use of two different metabolic pathways.

Furthermore, it was demonstrated that the senor functionality is not affected by OCP periods, i.e. periods without electroactive metabolic activity, up to 10 consecutive and 21 days in sum.

Concerning a practical application of the sensor this study revealed a good stability towards potential technical failures and showed reproducible signals in presence of different VFA. Both may also be of high relevance for other METs like MFCs. According to conceivable applications of the sensor as either online or offline sensor, the biphasic response behavior generates prerequisites for the storage of the sensor (offline sensor) or the process itself (online sensor). To reduce the latency of a prospective offline sensor, it should be stored at a high acetate concentration compared to the prospective process. As online sensor, the process should not possess distinct periods of low acetate concentrations. AD and wastewater-treatment, being among the main processes of interest, fulfil this requirement. However, a specific application as VFA-mix sensor in the AD process is temporarily hindered due to the reduction of the upper measurement range limit to ~2 mmol L^{-1}. In future this challenge will be tackled, e.g. by improved sensor architecture as well as dilution of process fluids.

Acknowledgments

Special thanks for excellent support to Desiree Schmidt by performing sequencing of the biofilms and to Anne Kuchenbuch who guided the T-RFLP analysis. J. K. acknowledges financial support by the Federal Ministry of Food and Agriculture (PhD student program of the Deutsches Biomasseforschungszentrum gemeinnützige GmbH). F. H. acknowledges support by the Federal Ministry of Education and Research (Research Award "Next generation biotechnological processes – Biotechnology 2020+") and the Helmholtz-Association (Young Investigators Group). This work was supported by the Helmholtz Association within the Research Program Renewable Energies and the Kurt Schwabe Institut für Mess- und Sensortechnik e.V. Meinsberg.

References

[1] D.R. Bond, D.R. Lovley, Electricity production by Geobacter sulfurreducens attached to electrodes, Appl. Environ. Microbiol. 69 (2003) 1548–1555, http://dx.doi.org/10.1128/AEM.69.3.1548-1555.2003.
[2] U. Schröder, F. Harnisch, L.T. Angenent, Microbial electrochemistry and technology: terminology and classification, Energy Environ. Sci. 8 (2015) 513–519, http://dx.doi.org/10.1039/C4EE03359K.
[3] G. Reguera, K.D. McCarthy, T. Mehta, J.S. Nicoll, M.T. Tuominen, D.R. Lovley, Extracellular electron transfer via microbial nanowires, Nature 435 (2005) 1098–1101, http://dx.doi.org/10.1038/nature03661.
[4] U. Schröder, Anodic electron transfer mechanisms in microbial fuel cells and their energy efficiency, Phys. Chem. Chem. Phys. 9 (2007) 2619–2629, http://dx.doi.org/10.1039/003627m.
[5] S.M. Strycharz-Glaven, R.M. Snider, A. Guiseppi-Elie, L.M. Tender, On the electrical conductivity of microbial nanowires and biofilms, Energy Environ. Sci. 4 (2011) 4366–4379, http://dx.doi.org/10.1039/C1EE01753E.
[6] N.S. Malvankar, M.T. Tuominen, D.R. Lovley, Lack of cytochrome involvement in long-range electron transport through conductive biofilms and nanowires of Geobacter sulfurreducens, Energy Environ. Sci. 5 (2012) 8651–8659, http://dx.doi.org/10.1039/C2EE22330A.
[7] E. Marsili, D.B. Baron, I.D. Shikhare, D. Coursolle, J.A. Gralnick, D.R. Bond, Shewanella secretes flavins that mediate extracellular electron transfer, Proc. Natl. Acad. Sci. U. S. A. 105 (2008) 3968–3973, http://dx.doi.org/10.1073/pnas.0710525105.
[8] J.M. Tront, J.D. Fortner, M. Plötze, J.B. Hughes, A.M. Puzrin, Microbial fuel cell biosensor for in situ assessment of microbial activity, Biosens. Bioelectron. 24 (2008) 586–590, http://dx.doi.org/10.1016/j.bios.2008.06.006.
[9] M. Di Lorenzo, T.P. Curtis, I.M. Head, K. Scott, A single-chamber microbial fuel cell as a biosensor for wastewaters, Water Res. 43 (2009) 3145–3154, http://dx.doi.org/10.1016/j.watres.2009.01.005.
[10] A. Kaur, J.R. Kim, I. Michie, R.M. Dinsdale, A.J. Guwy, G.C. Premier, Microbial fuel cell type biosensor for specific volatile fatty acids using acclimated bacterial communities, Biosens. Bioelectron. 47 (2013) 50–55, http://dx.doi.org/10.1016/j.bios.2013.02.033.
[11] Z. Liu, J. Liu, S. Zhang, X.-H. Xing, Z. Su, Microbial fuel cell based biosensor for in situ monitoring of anaerobic digestion process, Bioresour. Technol. 102 (2011) 10221–10229, http://dx.doi.org/10.1016/j.biortech.2011.08.053.
[12] Z. Liu, J. Liu, S. Zhang, Z. Su, Study of operational performance and electrical response on mediator-less microbial fuel cells fed with carbon- and protein-rich substrates, Biochem. Eng. J. 45 (2009) 185–191, http://dx.doi.org/10.1016/j.bej.2009.03.011.
[13] J. Kretzschmar, L.F.M. Rosa, J. Zosel, M. Mertig, J. Liebetrau, F. Harnisch, A microbial biosensor platform for in-line quantification of acetate in anaerobic digestion: potential and challenges, Chem. Eng. Technol. 39 (2016) 637–642, http://dx.doi.org/10.1002/ceat.201500406.
[14] W. Gujer, A.J.B. Zehnder, Conversion processes in anaerobic digestion, Water Sci. Technol. 15 (1983) 127–167.
[15] M.P. Bryant, E.A. Wolin, M.J. Wolin, R.S. Wolfe, Methanobacillus omelianskii, a symbiotic association of two species of bacteria, Arch. Für Mikrobiol. 59 (1967) 20–31, http://dx.doi.org/10.1007/BF00406313.
[16] M.J. Wolin, Interspecies transfer between H2-producing and methaneproducing species, in: H.G. Schlegel, G. Gottschalk, N. Pfenning (Eds.), Symp. Microb. Prod. Util. Gases, E. Goltz, Göttingen, Germany, 1975, pp. 141–150.
[17] P.L. McCarty, R.E. McKinney, Volatile acid toxicity in anaerobic digestion, J. Water Pollut. Control Fed. 33 (1961) 223–232.

[18] Marzano, Volatile fatty acids, an important state parameter for the control of the reliability and the productivities of methane anaerobic digestions, Biomass 1 (1981) 47–59.
[19] D.A. Stafford, The effects of mixing and volatile fatty acid concentrations on anaerobic digester performance, Biomass 2 (1982) 43–55, http://dx.doi.org/10.1016/0144-4565(82)90006-3.
[20] B.K. Ahring, M. Sandberg, I. Angelidaki, Volatile fatty acids as indicators of process imbalance in anaerobic digestors, Appl. Microbiol. Biotechnol. 43 (1995) 559–565, http://dx.doi.org/10.1007/BF00218466.
[21] D.G. Mulat, H.F. Jacobi, A. Feilberg, A.P.S. Adamsen, H.-H. Richnow, M. Nikolausz, Changing feeding regimes to demonstrate flexible biogas production: effects on process performance, microbial community structure and methanogenesis pathways, Appl. Environ. Microbiol. 82 (2) (2015) 438–449, http://dx.doi.org/10.1128/AEM.02320-15.
[22] E. Mauky, H.F. Jacobi, J. Liebetrau, M. Nelles, Flexible biogas production for demand-driven energy supply – feeding strategies and types of substrates, Bioresour. Technol. 178 (2015) 262–269, http://dx.doi.org/10.1016/j.biortech.2014.08.123.
[23] H. Hahn, B. Krautkremer, K. Hartmann, M. Wachendorf, Review of concepts for a demand-driven biogas supply for flexible power generation, Renew. Sustain. Energy Rev. 29 (2014) 383–393, http://dx.doi.org/10.1016/j.rser.2013.08.085.
[24] Y. Feng, X. Wang, B.E. Logan, H. Lee, Brewery wastewater treatment using air-cathode microbial fuel cells, Appl. Microbiol. Biotechnol. 78 (2008) 873–880, http://dx.doi.org/10.1007/s00253-008-1360-2.
[25] P. Clauwaert, W. Verstraete, Methanogenesis in membraneless microbial electrolysis cells, Appl. Microbiol. Biotechnol. 82 (2009) 829–836, http://dx.doi.org/10.1007/s00253-008-1796-4.
[26] R.K. Brown, F. Harnisch, S. Wirth, H. Wahlandt, T. Dockhorn, N. Dichtl, U. Schröder, Evaluating the effects of scaling up on the performance of bioelectrochemical systems using a technical scale microbial electrolysis cell, Bioresour. Technol. 163 (2014) 206–213, http://dx.doi.org/10.1016/j.biortech.2014.04.044.
[27] E.S. Heidrich, S.R. Edwards, J. Dolfing, S.E. Cotterill, T.P. Curtis, Performance of a pilot scale microbial electrolysis cell fed on domestic wastewater at ambient temperatures for a 12 month period, Bioresour. Technol. 173 (2014) 87–95, http://dx.doi.org/10.1016/j.biortech.2014.09.083.
[28] Z. Liu, J. Liu, B. Li, Y. Zhang, X.-H. Xing, Focusing on the process diagnosis of anaerobic fermentation by a novel sensor system combining microbial fuel cell, gas flow meter and pH meter, Int. J. Hydrog. Energy 39 (2014) 13658–13664, http://dx.doi.org/10.1016/j.ijhydene.2014.04.076.
[29] H. Liu, S. Cheng, B.E. Logan, Power generation in fed-batch microbial fuel cells as a function of ionic strength, temperature, and reactor configuration, Environ. Sci. Technol. 39 (2005) 5488–5493, http://dx.doi.org/10.1021/es050316c.
[30] S.A. Patil, F. Harnisch, B. Kapadnis, U. Schroeder, Electroactive mixed culture biofilms in microbial bioelectrochemical systems: the role of temperature for biofilm formation and performance, Biosens. Bioelectron. 26 (2010) 803–808, http://dx.doi.org/10.1016/j.bios.2010.06.019.
[31] S.A. Patil, F. Harnisch, C. Koch, T. Hübschmann, I. Fetzer, A.A. Carmona-Martínez, S. Müller, U. Schröder, Electroactive mixed culture derived biofilms in microbial bioelectrochemical systems: the role of pH on biofilm formation, performance and composition, Bioresour. Technol. 102 (2011) 9683–9690, http://dx.doi.org/10.1016/j.biortech.2011.07.087.
[32] X. Wang, S. Cheng, X. Zhang, X. Li, B.E. Logan, Impact of salinity on cathode catalyst performance in microbial fuel cells (MFCs), 2010, AsianAPEC BioH2 36 (2011) 13900–13906, http://dx.doi.org/10.1016/j.ijhydene.2011.03.052.
[33] G. Liu, S. Yu, H. Luo, R. Zhang, S. Fu, X. Luo, Effects of salinity anions on the anode performance in bioelectrochemical systems, Desalination 351 (2014) 77–81, http://dx.doi.org/10.1016/j.desal.2014.07.026.
[34] J.R. Kim, B. Min, B.E. Logan, Evaluation of procedures to acclimate a microbial fuel cell for electricity production, Appl. Microbiol. Biotechnol. 68 (2005) 23–30, http://dx.doi.org/10.1007/s00253-004-1845-6.
[35] C. Gimkiewicz, F. Harnisch, Waste water derived electroactive microbial biofilms: growth, maintenance, and basic characterization, J. Vis. Exp. 82 (2013), http://dx.doi.org/10.3791/50800.
[36] Y. Liu, F. Harnisch, K. Fricke, R. Sietmann, U. Schroeder, Improvement of the anodic bioelectrocatalytic activity of mixed culture biofilms by a simple consecutive electrochemical selection procedure, Biosens. Bioelectron. 24 (2008) 1006–1011, http://dx.doi.org/10.1016/j.bios.2008.08.001.
[37] C. Koch, A. Kuchenbuch, J. Kretzschmar, H. Wedwitschka, J. Liebetrau, S. Muller, F. Harnisch, Coupling electric energy and biogas production in anaerobic digesters – impacts on the microbiome, RSC Adv. 5 (2015) 31329–31340, http://dx.doi.org/10.1039/C5RA03496E.
[38] K.P. Nevin, H. Richter, S.F. Covalla, J.P. Johnson, T.L. Woodard, A.L. Orloff, H. Jia, M. Zhang, D.R. Lovley, Power output and columbic efficiencies from biofilms of Geobacter sulfurreducens comparable to mixed community microbial fuel cells, Environ. Microbiol. 10 (2008) 2505–2514, http://dx.doi.org/10.1111/j.1462-2920.2008.01675.x.
[39] C.I. Torres, R. Krajmalnik-Brown, P. Parameswaran, A.K. Marcus, G. Wanger, Y.A. Gorby, B.E. Rittmann, Selecting anode-respiring bacteria based on anode potential: phylogenetic, electrochemical, and microscopic characterization, Environ. Sci. Technol. 43 (2009) 9519–9524, http://dx.doi.org/10.1021/es902165y.
[40] P.G. Dennis, K. Guo, M. Imelfort, P. Jensen, G.W. Tyson, K. Rabaey, Spatial uniformity of microbial diversity in a continuous bioelectrochemical system, Bioresour. Technol. 129 (2013) 599–605, http://dx.doi.org/10.1016/j.biortech.2012.11.098.
[41] D. Segura, R. Mahadevan, K. Juárez, D.R. Lovley, Computational and experimental analysis of redundancy in the central metabolism of Geobacter sulfurreducens, PLoS Comput. Biol. 4 (2008) e36, http://dx.doi.org/10.1371/journal.pcbi.0040036.
[42] M. Aklujkar, J. Krushkal, G. DiBartolo, A. Lapidus, M.L. Land, D.R. Lovley, The genome sequence of Geobacter metallireducens: features of metabolism, physiology and regulation common and dissimilar to Geobacter sulfurreducens, BMC Microbiol. 9 (2009) 1–22, http://dx.doi.org/10.1186/1471-2180-9-109.
[43] G. Yang, S. Chen, S. Zhou, Y. Liu, Genome sequence of a dissimilatory Fe(III)-reducing bacterium Geobacter soli type strain GSS01T, Stand. Genom. Sci. 10 (2015) 1–10, http://dx.doi.org/10.1186/s40793-015-0117-7.
[44] D. Sun, A. Wang, S. Cheng, M. Yates, B.E. Logan, Geobacter anodireducens sp nov., an exoelectrogenic microbe in bioelectrochemical systems, Int. J. Syst. Evol. Microbiol. 64 (2014) 3485–3491, http://dx.doi.org/10.1099/ijs.0.061598-0.
[45] D. Sun, S. Cheng, A. Wang, F. Li, B.E. Logan, K. Cen, Temporal-spatial changes in viabilities and electrochemical properties of anode biofilms, Environ. Sci. Technol. (2015), http://dx.doi.org/10.1021/acs.est.5b00175.
[46] T. Yamashita, M. Ishida, S. Asakawa, H. Kanamori, H. Sasaki, A. Ogino, Y. Katayose, T. Hatta, H. Yokoyama, Enhanced electrical power generation using flame-oxidized stainless steel anode in microbial fuel cells and the anodic community structure, Biotechnol. Biofuels. 9 (2016), http://dx.doi.org/10.1186/s13068-016-0480-7.